Systems/Circuits

Statistics of Natural Communication Signals Observed in the Wild Identify Important Yet Neglected Stimulus Regimes in Weakly Electric Fish

Jörg Henninger,[1] Rüdiger Krahe,[2,3] Frank Kirschbaum,[2] Jan Grewe,[1] and Jan Benda[1]

[1]Institut für Neurobiologie, Eberhard Karls Universität, 72076 Tübingen, Germany, [2]Institut für Biologie, Humboldt-Universität zu Berlin, 10115 Berlin, Germany, and [3]McGill University, Department of Biology, Montreal, Quebec H3A 1B1, Canada

Sensory systems evolve in the ecological niches that each species is occupying. Accordingly, encoding of natural stimuli by sensory neurons is expected to be adapted to the statistics of these stimuli. For a direct quantification of sensory scenes, we tracked natural communication behavior of male and female weakly electric fish, *Apteronotus rostratus*, in their Neotropical rainforest habitat with high spatiotemporal resolution over several days. In the context of courtship, we observed large quantities of electrocommunication signals. Echo responses, acknowledgment signals, and their synchronizing role in spawning demonstrated the behavioral relevance of these signals. In both courtship and aggressive contexts, we observed robust behavioral responses in stimulus regimes that have so far been neglected in electrophysiological studies of this well characterized sensory system and that are well beyond the range of known best frequency and amplitude tuning of the electroreceptor afferents' firing rate modulation. Our results emphasize the importance of quantifying sensory scenes derived from freely behaving animals in their natural habitats for understanding the function and evolution of neural systems.

Key words: **animal communication; chirp; natural stimulus statistics; sexual dimorphism**

Significance Statement

The processing mechanisms of sensory systems have evolved in the context of the natural lives of organisms. To understand the functioning of sensory systems therefore requires probing them in the stimulus regimes in which they evolved. We took advantage of the continuously generated electric fields of weakly electric fish to explore electrosensory stimulus statistics in their natural Neotropical habitat. Unexpectedly, many of the electrocommunication signals recorded during courtship, spawning, and aggression had much smaller amplitudes or higher frequencies than stimuli used so far in neurophysiological characterizations of the electrosensory system. Our results demonstrate that quantifying sensory scenes derived from freely behaving animals in their natural habitats is essential to avoid biases in the choice of stimuli used to probe brain function.

Introduction

Sensory systems evolve in the context of species-specific natural sensory scenes (Lewicki et al., 2014). Therefore, naturalistic stimuli have been crucial for advances in understanding the design and function of neural circuits in sensory systems, in particular the visual system (Laughlin, 1981; Olshausen and Field, 1996; Gollisch and Meister, 2010; Froudarakis et al., 2014) and the auditory system (Theunissen et al., 2000; Smith and Lewicki, 2006; Clemens and Ronacher, 2013). Communication signals are natural stimuli that are, by definition, behaviorally relevant (Wilson, 1975; Endler, 1993). Not surprisingly, certain acoustic communication signals, for example, have been reported to evoke responses in peripheral auditory neurons that are highly informative about these stimuli (Rieke et al., 1995; Machens et al., 2005). However, other stimuli that do not strongly drive sensory

Received Feb. 7, 2018; revised March 12, 2018; accepted April 8, 2018.

Author contributions: J.H. wrote the first draft of the paper; J.H., R.K., J.G., and J.B. edited the paper. J.H., R.K., F.K., and J.B. designed research; J.H., R.K., F.K., J.G., and J.B. performed research; J.H. and J.B. analyzed data.

This work was supported by the German Federal Ministry of Education and Research (BMBF Bernstein Award for Computational Neuroscience 01GQ0802 to J.B.), the Natural Sciences and Engineering Research Council of Canada (Discovery Grant to R.K.), and the Smithsonian Tropical Research Institute (Short Time Fellowship to J.H.). We thank Hans Reiner Polder and Jürgen Planck from NPI Electronic GmbH for designing the amplifier; Sophie Picq, Diana Sharpe, Luis de León Reyna, Rigoberto González, Eldredge Bermingham, the staff from the Smithsonian Tropical Research Institute, and the Emberá community of Peña Bijagual for logistical support; Fabian Sinz for advice on the analysis; and Leonard Maler, Ulrich Schnitzler, and Janez Presern for comments on the manuscript.

The authors declare no competing financial interests.

Correspondence should be addressed to either Jan Benda or Jörg Henninger, Institut für Neurobiologie, Eberhard Karls Universität, Auf der Morgenstelle 28E, 72076 Tübingen, Germany, E-mail: jan.benda@uni-tuebingen.de or joerg.henninger@posteo.de.

DOI:10.1523/JNEUROSCI.0350-18.2018

 0270-6474/18/385456-11$15.00/0

neurons may also be behaviorally relevant and equally important for understanding the functioning of neural systems. Unfortunately, they are often neglected in electrophysiological studies because they do not evoke obvious neural responses (Olshausen and Field, 2005).

To address this bias, we quantified behaviorally relevant sensory scenes that we recorded in freely interacting animals in their natural habitat. Tracking the sensory input of freely behaving and unrestrained animals in natural environments is notoriously challenging (Egnor and Branson, 2016). We took advantage of the continuously generated electric organ discharge (EOD) (Fig. 1*A*) of gymnotiform weakly electric fish to track their movements and electrocommunication signals without the need for tagging individual fish.

The quasi-sinusoidal EOD, together with an array of electroreceptors distributed over the fish's skin (Carr et al., 1982), forms an active electrosensory system used for prey capture (Nelson and MacIver, 1999), navigation (Fotowat et al., 2013), and communication (Smith, 2013). Both the EOD alone and its modulations function as communication signals that convey information about species, sex, status, and intent of individuals (Hagedorn and Heiligenberg, 1985; Stamper et al., 2010; Fugère et al., 2011). In *Apteronotus*, several types of brief EOD frequency (EOD*f*) excursions called "chirps" (Fig. 1*B*) have been studied extensively in the laboratory setting (Engler and Zupanc, 2001) and have been associated with courtship (Hagedorn and Heiligenberg, 1985), aggression (Zakon et al., 2002), and the deterrence of attacks (Hupé and Lewis, 2008). P-unit tuberous electroreceptors encode amplitude modulations of the EOD (Bastian, 1981a) as they are induced by the presence of a second fish and by chirps (Benda et al., 2005; Walz et al., 2014).

Here, we describe electrocommunication behavior of weakly electric fish recorded in their natural Neotropical habitat with unprecedented high temporal and spatial resolution. We found extensive chirping interactions on timescales ranging from tens of milliseconds to minutes in the context of courtship. In a complementary breeding experiment, we confirmed the synchronizing role of chirping in spawning. From the observed courtship and aggression scenes, we computed the statistics of interaction distances determining the effective signal amplitudes and the signal frequencies driving the electrosensory system. In the discussion, we compare these natural stimulus statistics with the known coding properties of electroreceptor afferents.

Materials and Methods

Field site

The field site is located in the Tuira River basin, Province of Darién, Republic of Panamá (Fig. 1-1*A*, available at https://doi.org/10.1523/JNEUROSCI.0350-18.2018.f1-1), at Quebrada La Hoya, a narrow and slow-flowing creek supplying the Chucunaque River. Data were recorded ~2 km from the Emberá community of Peña Bijagual and ~5 km upstream of the stream's mouth (8° 15′ 13.50" N, 77° 42′ 49.40" W). At our recording site (Fig. 1-1*B*, available at https://doi.org/10.1523/JNEUROSCI.0350-18.2018.f1-1), the water level ranged from 20 cm at the slip-off slope to 70 cm at the cut bank. The water temperature varied between 25°C to 27°C on a daily basis and water conductivity was stable at 150–160 μS/cm. At this field site, we recorded four species of weakly electric fish, the pulse-type fish *Brachyhypopomus occidentalis* (~30–100 Hz pulses/s), the wave-type species *Sternopygus dariensis* (EOD*f* at ~40–220 Hz), *Eigenmannia humboldtii* (200–580 Hz), and *A. rostratus* (580–1100 Hz). We here focused exclusively on *A. rostratus*, a member of the *A. leptorhynchus* species group (brown ghost knifefish; de Santana and Vari, 2013).

Field monitoring system

Our recording system (Fig. 1*C* and Fig. 1-1*B*, available at https://doi.org/10.1523/JNEUROSCI.0350-18.2018.f1-1) consisted of a custom-built 64-channel electrode and amplifier system (NPI Electronics) running on 12 V car batteries. Electrodes were low-noise head stages encased in epoxy resin (1× gain, 10 × 5 × 5 mm). Signals detected by the head stages were fed into the main amplifier (100× gain, first-order high-pass filter 100 Hz, low-pass filter 10 kHz) and digitized with 20 kHz per channel with 16-bit amplitude resolution using a custom-built low-power-consumption computer with two digital-analog converter cards (PCI-6259; National Instruments). Recordings were controlled with custom software written in C++ (https://github.com/bendalab/fishgrid) that also saved data to hard disk for offline analysis (exceeding 400 GB of uncompressed data per day). We used a minimum of 54 electrodes arranged in a 9 × 6 array covering an area of 240 × 150 cm (30 cm spacing). The electrodes were mounted on a rigid frame (thermoplast 4 × 4 cm profiles, 60% polyamid, 40% fiberglass; Technoform Kunststoffprofile), which was submerged into the stream at the cut bank side and fixed in height 30 cm below the water level.

Data analysis

All data analysis was performed in Python 2.7 (www.python.org, https://www.scipy.org/). Scripts and raw data (Panamá field data: 2.0 TB, Berlin breeding experiment: 3.7 TB of EOD recordings and 11.4 TB video files) are available on request, data of the extracted EOD frequencies, position estimates, and chirps are available at https://doi.org/10.12751/g-node.87584d and some of the core algorithms are accessible at Github under the GNU general public license (https://github.com/bendalab/thunderfish).

Summary data are expressed as means ± SD unless indicated otherwise.

Spectrograms in Figures 3 and 7*B* were calculated from data sampled at 20 kHz in windows of 1024 and 2048 data points, respectively, and shifted by 50 data points.

Fish identification and tracking. First, information about electric fish presence, EOD*f*, and approximate position were extracted. Each electrode signal was analyzed separately in sequential overlapping windows (1.22 s width, 85% overlap). For each window, the power spectral density was calculated (8192 FFT data points, five subwindows, 50% overlap) and spectral peaks above a given threshold were detected. Individual fish were extracted from the list of peak frequencies based on the harmonic structure of wave-type EODs. Finally, fish detections in successive time windows were matched, combined, and stored for further analysis.

Based on EOD*f*, we separated male (EOD*f* > 750 Hz) from female fish (EOD*f* < 750 Hz) (Meyer et al., 1987). The data allowed us to analyze courtship and aggression of six male and two female fish in detail.

Position estimation. For each fish, the signals of all electrodes were band-pass filtered (forward–backward Butterworth filter, third order, 5× multipass, ±7 Hz width) at the fish's EOD*f*. Then, the envelope was computed from the resulting filtered signal using a root-mean-square filter (10 EOD cycles width). Each 40 ms the fish position $\vec{x}$ was estimated from the four electrodes i with the largest envelope amplitudes A_i at position $\vec{e}_i$ as a weighted spatial average (see Movie 1) as follows:

$$\vec{x} = \frac{\sum_{i=1}^{n=4} \sqrt{A_i} \cdot \vec{e}_i}{\sum_{i=1}^{n=4} \sqrt{A_i}}$$

This estimate proved to be the most robust against fish moving close to the edges of the electrode array, as verified with both experiments and simulations (Henninger, 2015). In short, we measured the spatial distribution of an electric fish's EOD field in a large tank (3.5 × 7.5 × 1.5 m, w × l × h) under conditions similar to field conditions (water depth 60 cm, fish and electrode array submerged 30 cm below surface). We used this dataset for evaluating the performance of three algorithms for position estimation and for fitting a simple dipole model for the spatial electric field distribution. The dipole model was then used to evaluate the algorithms in greater detail by simulating stationary and moving fish for various electrode configurations. For the electrode configuration used, the weighted spatial average yielded a precision of 4.2 ± 2.6 cm on level with the electrode array and 6.2 ± 3.8 cm at a vertical distance of 15 cm as

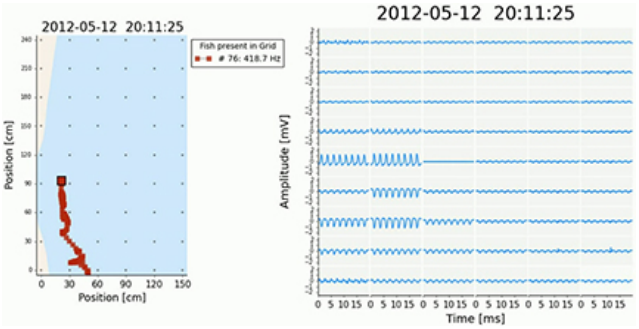

Movie 1. Example of raw voltage recordings and corresponding position estimates of a single fish, *E. humboldtii*, passing through the array of electrodes. The head and tail area of its electric field are of opposite polarity, which is why the polarity of the recorded EOD switches as the fish passes an electrode. Note the large electric spikes occurring irregularly on all electrodes. Previous studies (Hopkins, 1973) attributed similar patterns to propagating distant lightning. The animation is played back at real time.

computed by extensive simulations. Finally, the position estimates were filtered with a running average filter of 200 ms width to yield a smoother trace of movements.

Chirp detection and analysis. For each fish, the electrode voltage traces were bandpass-filtered (forward–backward Butterworth filter, third order, 5× multipass, ±7 Hz width) at the fish's EOD*f* and at 10 Hz above the EOD*f*. For each passband, the signal envelope was estimated using a root-mean-square filter over 10 EOD cycles. Rapid positive EOD*f* excursions cause the signal envelope at the fish's baseline frequency to drop and in the passband above the fish's EOD*f* to increase in synchrony with the frequency excursion. If events were detected synchronously in both passbands on more than two electrodes, and exceeded a preset amplitude threshold, they were accepted as communication signals.

Communication signals with a single peak in the upper passband were detected as small chirps. Signals of up to 600 ms duration and two peaks in the upper passband, marking the beginning and the end of the longer frequency modulation, were detected as long chirps. All chirps in this study were verified manually. However, it is likely that some chirps were missed, since detection thresholds were set such that the number of false positives was very low. In addition, abrupt frequency rises (Engler and Zupanc, 2001) were probably not detected because of their low-frequency increase.

Interchirp interval probability densities were generated for pairs of fish and only for the time period in which both fish were producing chirps. Kernel density histograms of interchirp intervals (Fig. 5-1, available at https://doi.org/10.1523/JNEUROSCI.0350-18.2018.f5-1) were computed with a Gaussian kernel with an SD of 20 ms.

Rates of small chirps before and after female long chirps (see Fig. 5*A*, *C*) were calculated by convolving the chirp times with a Gaussian kernel ($\sigma = 0.5$ s) separately for each episode and subsequently calculating the means and SDs.

For quantifying the echo response (see Fig. 6), we computed the cross-correlogram as follows:

$$r(\tau) = \frac{1}{n_a} \sum_{j=1}^{n_a} \sum_{i=1}^{n_b} g(\tau - (t_{b,i} - t_{a,j}))$$

with the n_a chirp times $t_{a,j}$ of fish *a* and the n_b chirp times $t_{b,i}$ of fish *b* using a Gaussian kernel $g(t)$ with a SD of 20 ms. To estimate its confidence intervals, we repeatedly resampled the original dataset (2000 times jackknife bootstrapping; random sampling with replacement), calculated the cross-correlogram as described above, and determined the 2.5% and 97.5% percentiles. To create the cross-correlograms of independent chirps, we repeatedly (2000 times) calculated the cross-correlograms on chirps jittered in time by adding a random number drawn from a Gaussian distribution with a SD of 500 ms and determined the mean and the 2.5% and 97.5% percentiles. Deviations of the observed cross-correlogram beyond the confidence interval of the cross-correlogram of jittered chirp times are significant on a 5% level and are indicative of an echo response. Reasonable numbers of chirps for computing meaningful cross-correlograms (more than several hundreds of chirps) were available in five pairs of fish.

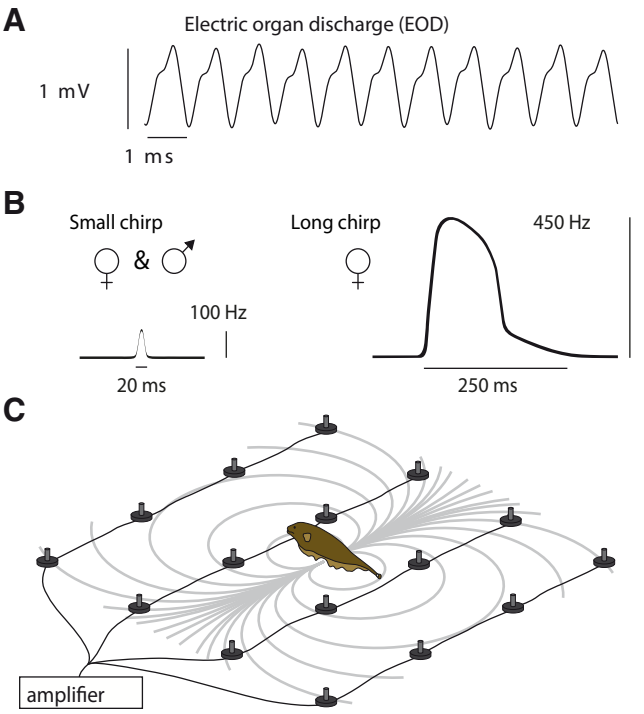

Figure 1. Monitoring electrocommunication behavior in the natural habitat. ***A***, EOD waveform of *A. rostratus*. ***B***, Transient increases of EOD*f*, called small and long chirps, function as communication signals. ***C***, The EOD generates a dipolar electric field (gray isopotential lines) that we recorded with an electrode array, allowing us to track individual fish and to monitor communication interactions with high temporal and spatial acuity. Figure 1-1, available at https://doi.org/10.1523/JNEUROSCI.0350-18.2018.f1-1, shows the location of our field site and the electrode array submerged in a small stream in Panama.

Beat frequencies and spatial distances. The distance between two fish at the time of each chirp (Fig. 8*B*) was determined from the estimated fish positions. As the receiver of the chirp, we assigned the fish that was closest to the sender and at maximum 150 cm away. The distance estimates were compiled into kernel density histograms that were normalized to their maximal value. The Gaussian kernel had a SD of 1 cm for courtship small chirps and 2 cm for courtship long chirps and intruder small chirps. Distances between the intruding male and the courting male during assessment behavior (Fig. 8*C*, top) were measured every 40 ms beginning with the appearance of the intruding fish until the eventual approach or attack. These distances, collected from a total assessment time of 923 s, were summarized in a kernel density histogram with Gaussian kernels with a SD of 2 cm.

Based on the results and procedures from Figure 8*B*, we defined "courting dyads" as pairs in which a male fish chirped at a female within a range of 60 cm.

Attack distances between two males (Fig. 8*C*, bottom) were determined at the moment a resident male initiated its movement toward an intruding male. This moment was clearly identifiable as the onset of a linear movement of the resident male toward the intruder from plots showing the position of the fish as a function of time.

The distribution of beat frequencies generated by fish present in the electrode array at the same time (Fig. 8*E*) was calculated from all recordings. The average frequency difference of each pair of fish simultaneously detected in the recordings was compiled into a kernel density histogram with a Gaussian kernel with a SD of 10 Hz. Similarly, for courtship and aggressive behavior (Fig. 8*F*, *G*), the mean frequency differences were extracted for the duration of these interactions.

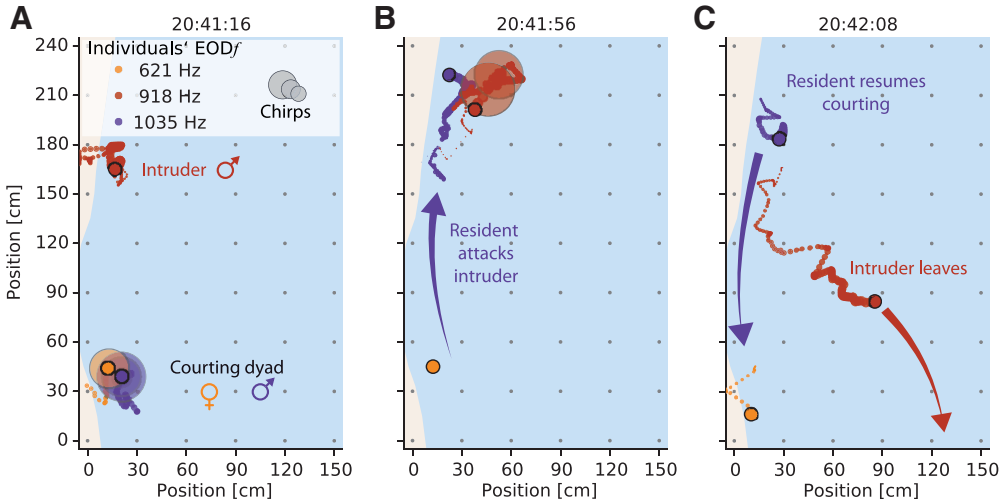

Figure 2. Snapshots of reconstructed interactions of weakly electric fish. See Movie 2 for an animation. The current fish position is marked by filled circles. Trailing dots indicate the positions over the preceding 5 s. Individual fish are labeled by the same colors across all figures. Large transparent circles denote occurrence of chirps. Gray dots indicate electrode positions and light blue illustrates the water surface. The direction of water flow is from top to bottom. ***A***, Courting female (orange) and male (purple) are engaged in intense chirping activity. An intruder male (red) lingers at a distance of ~1 m. ***B***, ***C***, The courting male attacks (purple arrow) the intruder (***B***), who emits a series of chirps and leaves the recording area (***C***, red arrow) while the resident male resumes courting (***C***, purple arrow).

Movie 2. Animation of courtship and aggression behaviors. The animation is played back at 2× real time.

Electric fields. For an estimation of EOD amplitude as a function of distance, histograms of envelope amplitudes from all electrodes of the array were computed as a function of distance between the electrodes and the estimated fish position. For each distance bin in the range of 20–100 cm, the upper 95% percentile of the histogram was determined and a power law was fitted to these data points. Gymnotiform electroreceptors measure the electric field; that is, the first spatial derivative of the EOD amplitudes, as shown in Figure 8*A*.

Breeding monitoring setup

In the laboratory breeding study, we used the brown ghost knifefish *A. leptorhynchus*, a close relative of *A. rostratus* (de Santana and Vari, 2013). The two species share many similarities: most chirps produced by both species are "small chirps" that in *A. leptorhynchus* have been classified as type 2 chirps (Engler and Zupanc, 2001), females of both species additionally generate small proportions of "long chirps" similar to the type 4 chirps classified for *A. leptorhynchus* males, and both species show the same sexual dimorphism in EOD*f*.

The laboratory setup for breeding *A. leptorhynchus* consisted of a tank (100 × 45 × 60 cm) placed in a darkened room and equipped with bubble filters and PVC tubes provided for shelter. Water temperature was kept between 21°C and 30°C. The light/dark cycle was set to 12/12 h. Several pieces of rock were placed in the center of the tank as spawning substrate. EOD signals were recorded differentially using four pairs of graphite electrodes. Two electrode pairs were placed on each side of the spawning substrate. The signals were amplified and analog filtered using a custom-built amplifier (100× gain, 100 Hz high-pass, 10 kHz low-pass; NPI Electronics), digitized at 20 kHz with 16 bit (PCI-6229, National Instruments), and saved to hard disk for offline analysis. The tank was illuminated at night with a dozen infrared LED spotlights (850 nm, 6 W, ABUS TV6700) and monitored continuously (Movie 4) with two infrared-sensitive high-resolution video cameras (Logitech HD webcam C310, IR filter removed manually). The cameras were controlled with custom-written software (https://github.com/bendalab/videoRecorder) and a timestamp for each frame was saved for later synchronization of the cameras and EOD recordings. Six fish of *A. leptorhynchus* (three male, three female; imported from the Río Meta region, Colombia) were kept in a tank for 1 year before being transferred to the recording tank. First, fish were monitored for ~1 month without external interference. We then induced breeding conditions (Kirschbaum and Schugardt, 2002) by slowly lowering water conductivity from 830 to ~100 μS/cm over the course of 3 months by diluting the tank water continuously with deionized water. The tank was monitored regularly for the occurrence of spawned eggs.

Results

We recorded the EODs of weakly electric fish in a stream in the Panamanian rainforest by means of a submerged electrode array at the onset of their reproductive season in May of 2012 (Fig. 1*C*, Fig. 1-1, available at https://doi.org/10.1523/JNEUROSCI.0350-18.2018.f1-1, Movie 1). Individual gymnotiform knifefish, *A. rostratus*, were identified and their movements tracked continuously based on the species- and individual-specific frequency of their EOD (EOD*f* ≈580–1050 Hz). In these recordings, we detected several types of "chirps" emitted during courtship and aggression (Fig. 1*B*). This approach allowed us to reconstruct social interactions in detail (Fig. 2, Movie 2 and 3) and to evaluate the associated sensory scenes experienced by these fish in their natural habitat.

Electrocommunication in the wild

We focused on two relevant communication situations, courtship and aggressive dyadic interactions. In total, we detected 54 episodes of short-distance interactions that we interpreted as courtship (see below) between low-frequency females (EOD*f* < 750 Hz, $n = 2$) and high-frequency males (EOD*f* > 750 Hz, $n = 6$) (Meyer et al., 1987), occurring in 2 of 5 nights. Courting was characterized by extensive production of chirps (Fig. 2*A*, 3) by both males and females, with up to 8400 chirps per individual per night (Fig. 4). Most chirps were so-called "small chirps," characterized by short duration (<20 ms) EOD*f* excursions of <150 Hz and a minimal reduction in EOD amplitude (Engler and Zupanc, 2001) (Figs. 1*B*, 3). Only females emitted an additional type of

chirp in courtship episodes, the "long chirp" (Figs. 1*B*, 3), with a duration of 162 ± 39 ms (n = 54), a large EOD*f* excursion of ~400 Hz, and a strong decrease in EOD amplitude (Hagedorn and Heiligenberg, 1985). Per night and female, we observed 9 and 45 long chirps, respectively, generated every 3–9 min (first and third quartile) between 7:00 P.M. 1:00 A.M. (Fig. 4*A*). Occasionally, courtship was interrupted by intruding males, leading to aggressive interactions between resident and intruder males (see below).

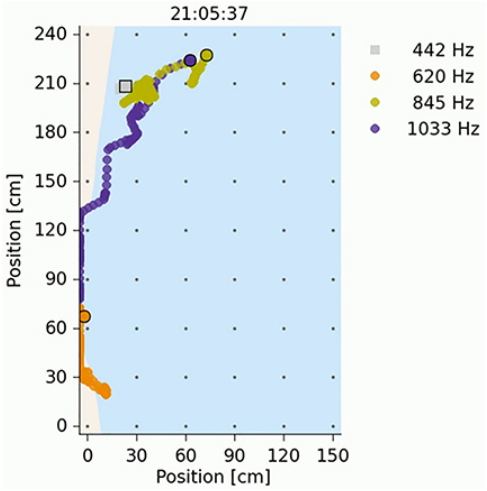

Movie 3. Animation of a courtship sequence with multiple attempts of an intruding male to approach the courting dyad. The resident male drives the intruder away three times, starting the approach at increasingly greater distances. *A. rostratus* are marked by circles, *E. humboldtii* by squares. The animation is played back at 2× real time.

Courtship chirping

Roaming males approached and extensively courted females by emitting large numbers of small chirps (Fig. 4*A*). Courtship communication was highly structured, with female long chirps playing a central role. Long chirps were preceded by persistent emission of small chirps by the male with rates of up to 3 Hz (Fig. 5*A*,*C*, and Fig. 5-2, available at https://doi.org/10.1523/JNEUROSCI.0350-18.2018.f5-2). Immediately before the long chirp, the female small-chirp rate tripled from below 1 to ~3 Hz within a few seconds. The male chirp rate followed this increase until the concurrent high-frequency chirping of both fish ceased after the female long chirp. These chirp episodes were characterized by close proximity of the two fish (<30 cm; Fig. 5*B*,*D*). Long chirps were consistently acknowledged by males with a doublet of small chirps (Fig. 3) emitted 229 ± 31 ms after long chirp onset (n = 53 measured in 5 pairs of interacting fish; Fig. 4*A*). The two chirps of the doublet were separated by only 46 ± 6 ms, 7-fold shorter than the most prevalent chirp intervals (Fig. 5-1, available at https://doi.org/10.1523/JNEUROSCI.0350-18.2018.f5-1). Finally, the female often responded with a few more loosely timed small chirps ~670 ± 0.182 ms after the long chirp (time of first chirp observed in n = 33 of the 40 episodes shown in Fig. 5-2, available at https://doi.org/10.1523/JNEUROSCI.0350-18.2018.f5-2). The concurrent increase in chirp rate, its termination by the female long chirp, the male doublet, and the final response by small chirps of the female stood out as a highly stereotyped communication motif that clearly indicates fast interactive communication.

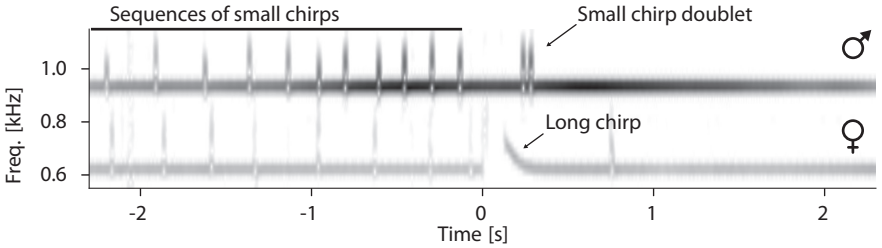

Figure 3. Spectrogram of stereotyped courtship chirping. The example spectrogram (Audio 1) shows EOD*f*s of a female (620 Hz, same as in Fig. 2) and a male (930 Hz) and their stereotyped chirping pattern during courtship: the two fish concurrently produce series of small chirps before the female generates a long chirp. The long chirp is acknowledged by the male with a chirp doublet that in turn is often followed by one or more small chirps emitted by the female. For statistics, see text, Figure 5, Figure 5-2, available at https://doi.org/10.1523/JNEUROSCI.0350-18.2018.f5-2, and Figure 6.

Males echo female chirps

On a subsecond timescale, male chirping was modulated by the timing of female chirps (Fig. 6*A*,*C*). After a female small chirp, male chirp probability first decreased to a minimum at ~75 ms (significant in 4 of 5 pairs of fish) and subsequently increased to a peak at ~165 ms (significant in 4 of 5 pairs of fish). In contrast to males, females did not show any echo response (Fig. 6*B*,*D*); they timed their chirps independently of the males' chirps.

Competition between males

A second common type of electrocommunication interaction observed in our field data was aggressive encounters between males competing for access to reproductively active females. These aggressive interactions were triggered by intruding males that disrupted courtship of a resident, courting dyad. Intruding males initially often lingered at distances larger than 70 cm from the courting dyad (8 of 16 scenes, median duration 58.5 s; for examples, see Fig. 2*A*, Movie 2), consistent with assessment behavior (Arnott and Elwood, 2008). Resident males detected and often attacked intruders over distances of up to 177 cm, showing a clear onset of directed movement toward the intruder (Fig. 2*C*, Movie 2). In 5 of 12 such situations, a few small chirps indistinguishable from those produced during courtship were emitted exclusively by the retreating fish (Fig. 4*A*). The distances at which resident males started to attack intruders ranged from 20 to 177 cm (81 ± 44 cm, n = 10; Fig. 2*B*, Movie 3). At the largest observed attack distance of 177 cm, the electric field strength was estimated to be maximally 0.34 μV/cm (assuming the fish were oriented optimally), a value close to minimum behavioral threshold values of ~0.3–0.1 μV/cm measured in the laboratory at the fish's best frequency (Bullock et al., 1972; Knudsen, 1974). We observed a single rise: a slow, gradual increase in EOD*f* (Zakon et al., 2002) emitted by a retreating intruder fish.

Synchronization of spawning

We investigated the role of the female long chirp in a breeding experiment in the laboratory (Kirschbaum and Schugardt, 2002) by recording and videotaping a group of 3 males and 3 females of the closely related species *A. leptorhynchus* (de Santana and Vari, 2013) continuously over >5 months. Scanning >1.3 million emitted chirps, we found 76 female long chirps embedded in communication episodes closely similar to those observed in *A.*

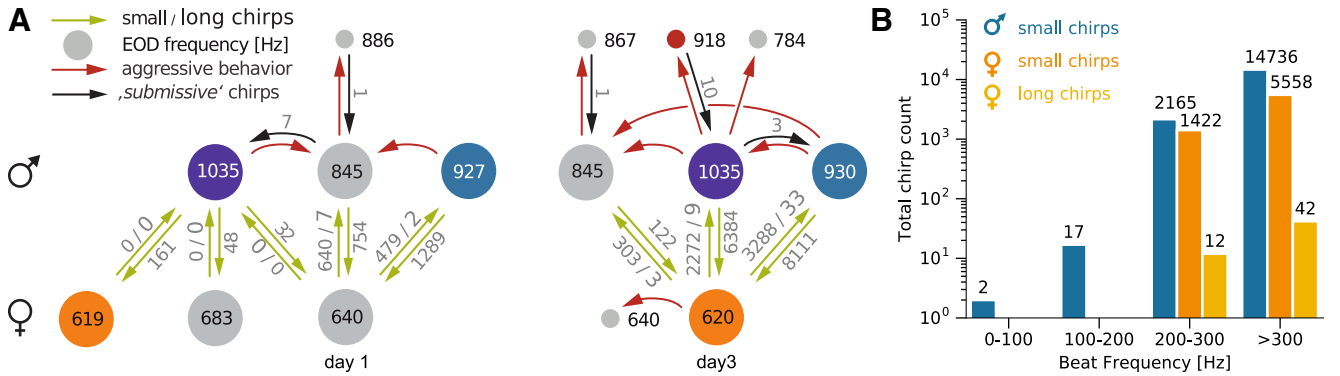

Figure 4. Social interactions and chirping. ***A***, Ethogram of interactions of *A. rostratus* individuals (colored circles). The ethogram is based on data from 2012-05-10 (night 1) and 2012-05-12 (night 3) and illustrates the number and EOD frequencies of interacting fish as well as the number of emitted chirps that have been analyzed in this study. The numbers within circles indicate the EOD*f*s of each fish in Hertz. Fish with similar EOD*f*s on day 1 and day 3 may have been the same individuals. Green arrows and associated numbers indicate the numbers of small chirps and long chirps emitted in close proximity (<50 cm). Red arrows indicate aggressive behaviors and black arrows the number of small chirps emitted during aggressive interactions. ***B***, Histogram of chirp counts as a function of beat frequency (bin width: 100 Hz). Note logarithmic scale used for chirp counts.

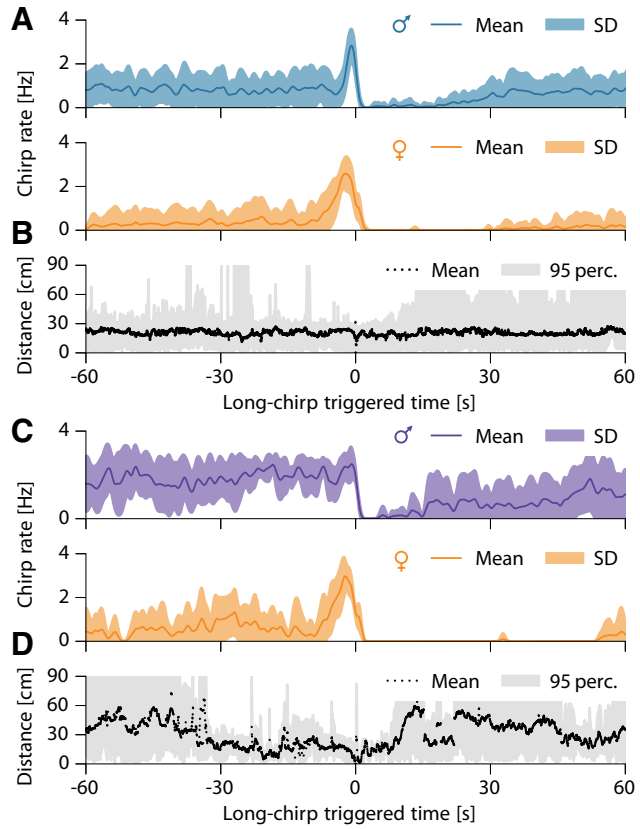

Figure 5. Temporal structure of courtship chirping of two example pairs. ***A***, Average rate of small chirps of a male (top, EOD*f* = 930 Hz) courting a female (bottom, EOD*f* = 620 Hz, *n* = 32 episodes, same pair as in Fig. 3, beat frequency is 310 Hz). ***B***, Corresponding distance between the courting male and female. ***C***, ***D***, Same as in ***A*** and ***B*** for the pair shown in Figure 2 (same female as in ***A*** and ***B***, male EOD*f* = 1035 Hz, beat frequency 415 Hz, *n* = 8 episodes). Time 0 marks the female long chirp. Bands mark 95% percentiles. See Figure 5-1, available at https://doi.org/10.1523/JNEUROSCI.0350-18.2018.f5-1, for corresponding interchirp-interval distributions and Figure 5-2, available at https://doi.org/10.1523/JNEUROSCI.0350-18.2018.f5-2, for corresponding raster plots of small chirps.

rostratus in the wild (cf. Figs. 7*B*, 3). Eggs were only found after nights with long chirps (six nights). The number of eggs found corresponded approximately to the number of observed long chirps, supporting previous anecdotal findings that *Apteronotus* females spawn single eggs during courtship episodes (Hagedorn and Heiligenberg, 1985). The associated video sequences triggered on female long chirps show that, before spawning, females swim on their side close to the substrate, such as a rock or a filter, whereas the male hovers in the vicinity of the female and emits chirps continuously (Movie 4). In the last seconds before spawning, the female starts to emit a series of chirps, whereupon the male approaches the female. A fraction of a second before the female emits its long chirp, the male pushes the female and retreats almost immediately afterward (Fig. 7). It seems highly likely that this short episode depicts the synchronized release of egg and sperm.

Statistics of natural stimuli

In a final step, we deduced the statistics of natural electrosensory stimuli resulting from the observed communication behaviors of *A. rostratus* to be able to relate it to the known physiological properties of electrosensory neurons in the discussion. Superposition of a fish's EOD with that of a nearby fish results in a periodic amplitude modulation, a so-called beat. Both frequency and amplitude of the beat provide a crucial signal background for the neural encoding of communication signals (Benda et al., 2005; Marsat et al., 2012; Walz et al., 2014). The beat frequency is given by the difference between the two EOD*f*s and the beat amplitude equals the EOD amplitude of the nearby fish at the position of the receiving fish (Fotowat et al., 2013).

The EOD amplitude and thus the beat amplitude decay with distance. We measured this decay directly from the data recorded with the electrode array (Fig. 8*A*). The median EOD field amplitude at 3 cm distance was 2.4 mV/cm (range 1.4–5.1). The electric field decayed with distance according to a power law with exponent 1.28 ± 0.12 (n = 9). This is less than the exponent of 2 expected for a dipole, because the water surface and the bottom of the stream distort the field (Fotowat et al., 2013). Small and long chirps emitted during courtship and small chirps emitted by retreating intruder males occurred at small distances of <32 cm (Fig. 8*B*). In contrast, two behaviors involving intruding males occurred at large distances (Fig. 8*C*). First, intruding males initially often lingered at distances larger than 70 cm from the courting dyad (n = 8, median duration 58.5 s; for examples, see Fig. 2*A*, Movie 2), consistent with assessment behavior (Arnott and Elwood, 2008). Second, the distances at which resident males started to attack intruders ranged from 20 to 177 cm (81 ± 44 cm, n = 10; Fig. 2*B*, Movie 3). At the largest observed attack distance

of 177 cm, we estimated the electric field strength to be maximally 0.34 μV/cm, assuming the fish were oriented optimally.

All courtship chirping occurred at high beat frequencies (205–415 Hz for the five pairs in which the female emitted long chirps; Figs. 8*F*, 4*B*). High beat frequencies were not a rare occurrence, as the probability distribution of 406 beat frequencies measured from encounters in five nights show (Fig. 8*E*). From these, the 183 male–female encounters resulted in beat frequencies ranging from 99 to 415 Hz. Conversely, same-sex interactions resulted in low beat frequencies up to 245 Hz (Fig. 8*E*). Encounters between females were more frequent than between males (187 female vs 36 male encounters). Female EOD*f*s ranged from 585 to 748 Hz and resulted in observed beat frequencies from 1 to 142 Hz. Beat frequencies of 49 Hz were the most frequent among the females ($n = 187$). Conversely, male EOD*f*s spanned a much larger range from 776 to 1040 Hz, resulting in a broad and flat distribution of beat frequencies spanning 12 to 245 Hz (peak at 98 Hz, $n = 36$). This includes the range of beat frequencies observed at aggressive male–male interactions (Fig. 8*G*).

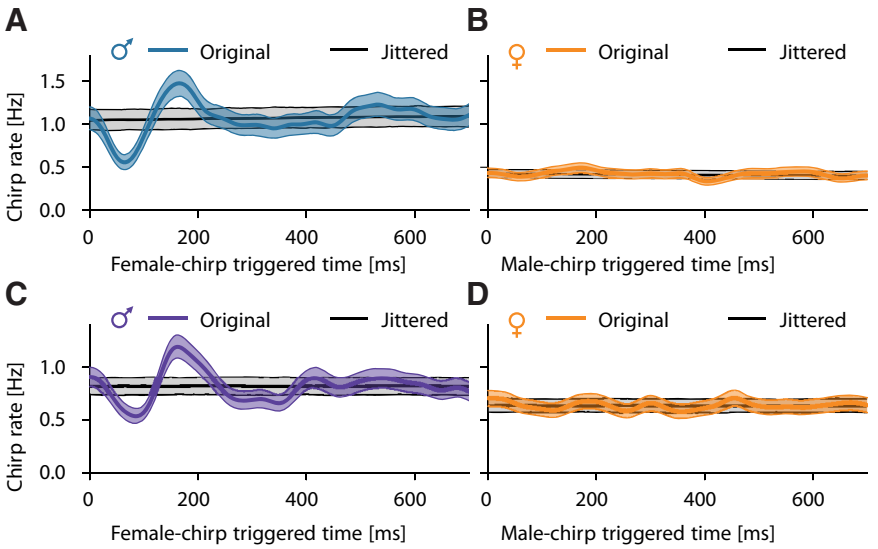

Figure 6. Fine structure of courtship chirping. Shown are cross-correlograms of chirp times; that is, the chirp rate of one fish relative to each chirp of the other fish (median with 95% confidence interval in color), of the same courting pairs of fish as in Figure 5. Corresponding chirp rates and confidence intervals from randomly jittered, independent chirp times are shown in gray. ***A***, ***C***, Male chirping is first significantly inhibited immediately after a female chirp (***A***: at 64 ms, Cohen's $d = 9.3$, $n = 2565$ female chirps, ***C***: at 85 ms, Cohen's $d = 7.1$, $n = 3213$ female chirps) and then transiently increased (***A***: at 166 ms, $d = 5.9$, ***C***: at 162 ms, $d = 7.5$). ***B***, ***D***, Female chirps are timed independently of male chirps (***B***: maximum $d = 2.8$, $n = 2648$ male chirps, ***D***: maximum $d = 1.9$, $n = 2178$ male chirps).

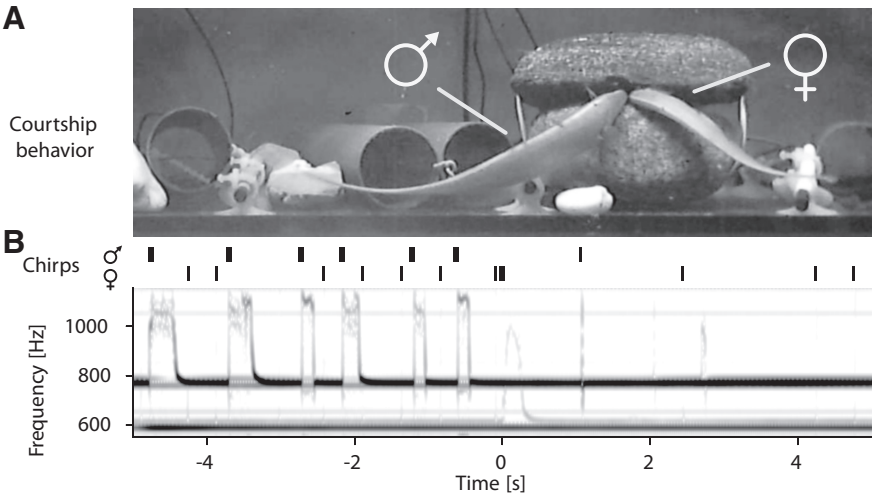

Figure 7. Synchronizing role of the female long chirp in spawning. ***A***, ***B***, Simultaneous video (***A***; snapshot of Movie 4) and voltage recordings (***B***; spectrogram) of *A. leptorhynchus* in the laboratory demonstrate the synchronizing function of the female long chirp (at time 0; trace with EOD$f = 608$ Hz baseline frequency) in spawning. In contrast to *A. rostratus*, male *A. leptorhynchus* generate an additional, long chirp type before spawning (top trace with EOD$f = 768$ Hz baseline frequency). Chirp onset times of the male and the female are marked by vertical bars above the spectrogram. Thick and thin lines indicate long and short duration chirps, respectively.

Movie 4. Spawning of the closely related species *A. lepthorhynchus* during a breeding experiment. The overall sequence of chirp production is very similar to the courtship motif observed in *A. rostratus*. However, male *A. lepthorhynchus* increasingly generate a second type of chirp, a variety of a long chirp, as spawning approaches. The video shows a big male (EOD$f = 770$ Hz) courting a smaller female (590 Hz). The audio signal was created from concurrent EOD recordings. Both fish generate chirps at an increased rate (~1.5 Hz) just before the male thrusts its snout against the female, which responds with a long chirp clearly noticeable from the audio trace. Subsequently, the male retreats to a tube and the female hovers around the substrate, where the spawned egg was found.

Discussion

We recorded movement and electrocommunication signals in a wild population of the weakly electric fish, *A. rostratus*, in their natural Neotropical habitat. A stereotyped pattern of interactive chirping climaxed in a special long chirp emitted by the female that we identified as a synchronizing signal for spawning. Courtship chirping was characterized by concurrent increases in chirp rate of both males and females on a tens-of-seconds time scale and by echo responses by the males on a 100 ms time scale. Courtship chirping occurred at distances below 32 cm and on high beat frequencies of up to 415 Hz. In contrast, aggressive interactions between males occurred at beat frequencies below ~200 Hz and often at distances larger than half a meter.

Communication in the wild and in the laboratory

Our observations of male echo responses to female chirps (Fig. 6*A*,*C*), precisely timed chirp doublets in response to female long chirps (Fig. 3), immediate behavioral reactions of males to female long chirps (Fig. 7, Movie 4), and females slowly raising their chirp rate in response to male chirping and responding to the male's chirp doublet (Fig. 5 and Fig. 5-2, available at https://doi.org/10.1523/JNEUROSCI.0350-18.2018.f5-2) clearly qualify chirps as communication signals in natural conditions. Laboratory studies have found echo responses on similar (Hupé and Lewis, 2008) or slower (Zupanc et al., 2006; Salgado and Zupanc, 2011; Metzen and Chacron, 2017) time scales exclusively between

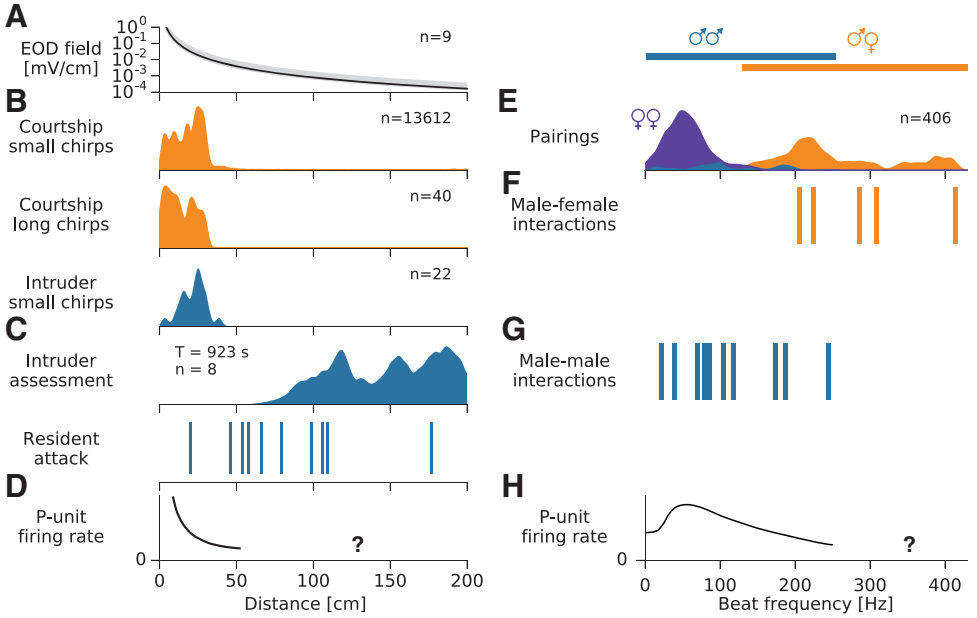

Figure 8. Statistics of behaviorally relevant natural stimuli. ***A***, Maximum electric field strength as a function of distance from the emitting fish (median with total range). ***B***, Small and long chirps in both courtship and aggression contexts are emitted consistently at distances below 32 cm. ***C***, Intruder assessment and initiation of attacks by residents occur at much larger distances (Movie 3). ***D***, Population-averaged firing rate response of P-unit afferents quickly decays with distance (sketch based on data from Bastian, 1981a, Fig. 6). Responses to stimulus amplitudes corresponding to distances larger than ~50 cm have not been measured yet (indicated by question mark). ***E***, Distribution of beat frequencies of all *A. rostratus* appearing simultaneously in the electrode array. Blue, male–male; violet, female–female; orange, male–female ($n = 406$ pairings). ***F***, Courtship behaviors involving small and long chirps occurred at beat frequencies in the range of 205–415 Hz. ***G***, Male–male interactions involving small chirps emitted by an intruder, intruder assessment, and attacks occurred at beat frequencies below 245 Hz. ***H***, Sketch of the tuning to beat frequencies of population-averaged firing-rate responses of P-unit afferents based on Scheich et al. (1973), Bastian (1981a), Nelson et al. (1997), Benda et al. (2005), and Walz et al. (2014). Almost nothing is known about responses to beat frequencies beyond 300 Hz (indicated by question mark). The data reported by Savard et al. (2011) on stimulus–response coherences and by Sinz et al. (2017) on spike time locking are the only exceptions (see Discussion).

males. Small chirps have been suggested to deter aggressive behavior (Hupé and Lewis, 2008). This is consistent with our observation of a submissive function of male–male chirping. The number of chirps generated in these aggressive contexts is, however, much lower (1–10 chirps in 5 of 9 pairings; Fig. 4) compared with encounters staged in laboratory tanks (~125 chirps per 5 min trial; Hupé and Lewis, 2008). Our field data do not support a function of chirps as signals of aggression and dominance (Triefenbach and Zakon, 2008). In particular, the restricted space in laboratory experiments may explain these differences.

In so-called "chirp chamber" experiments, in which a fish is restrained in a tube and is stimulated with artificial signals mimicking conspecifics, small chirps are predominantly generated by males at beat frequencies well below ~150 Hz, corresponding to same-sex interactions (Bastian et al., 2001; Engler and Zupanc, 2001). In contrast, in our observations of courting fish in the field and in the laboratory, both male and female fish almost exclusively chirped in male–female contexts at beat frequencies above ~200 Hz (Fig. 4*B*).

Electric synchronization of spawning by courtship-specific chirps

Our results provide strong evidence that female long chirps are an exclusive communication signal for the synchronization of egg and sperm release for external fertilization as has been suggested by Hagedorn and Heiligenberg (1985). The female long chirp was the central part of a highly stereotyped communication pattern between a courting dyad (Figs. 3, 5, and 5-2, available at https://doi.org/10.1523/JNEUROSCI.0350-18.2018.f5-2). Fertilized eggs were found at the locations of male–female interactions and only when the female had produced long chirps in the preceding night. The period immediately before the female long chirp was characterized by extensive chirp production by the male (Fig. 5). Video sequences triggered on female long chirps clearly demonstrated the special role of the female long chirp (Fig. 7, Movie 4). The videos also show that, in the seconds before emission of the long chirp, the fish were in very close proximity. Therefore, additional cues such as high beat amplitudes and touch might also play a role in synchronization of fertilization.

Robust responses to communication signals

Male echo responses to female chirps occurring reliably within a few tens of milliseconds (Fig. 6*A*,*C*), precisely timed chirp doublets (Fig. 3), and long-range assessment and attacks (Fig. 8*C*) demonstrate that the respective electrocommunication signals are successfully and robustly evaluated by the electrosensory system, as would be expected for communication signals (Wilson, 1975; Endler, 1993). The electrosensory signals arising in these interactions are dominated by beats; that is, amplitude modulations arising from the interference of the individual electric fields.

Two types of tuberous electroreceptor afferents could contribute to the observed behavioral responses in *A. rostratus*. T-units play an important role in the jamming avoidance response (Bullock et al., 1972; Rose and Heiligenberg, 1985). However, whether and how T-units are able to encode beats with frequencies >20 Hz is not yet known. P-units, the dominant type of tuberous receptors (Carr et al., 1982), encode amplitude modulations of the fish's EOD by modulating their firing rate (Scheich et al., 1973; Bastian, 1981a; Nelson et al., 1997; Benda et al., 2005; Walz et al., 2014). Tuning of P-unit firing-rate modulations, spike time correlations, and stimulus–response coherences to beat frequencies have been characterized up to beat frequencies

of 300 Hz by single-unit, dual-unit, and nerve recordings (Bastian, 1981a; Nelson et al., 1997; Benda et al., 2006; Walz et al., 2014). These measures are on average strongest at beat frequencies of ~30 to 130 Hz (Bastian, 1981a; Benda et al., 2006; Walz et al., 2014; Grewe et al., 2017), covering well the beat frequencies arising from same-sex interactions (Fig. 8*G*). For higher beat frequencies, firing-rate modulations and related measures decay down to lower values (Fig. 8*H*). Encoding of low beat frequencies occurring during male–male interactions is thus well understood.

Neglected stimulus frequencies

Only very few studies have looked at P-unit responses to beat frequencies beyond 300 Hz and none has addressed the encoding of chirps beyond 250 Hz. Narrow-band amplitude modulations of up to 400 Hz were shown to evoke sizable stimulus–response coherences (Savard et al., 2011). Based on our findings from this field study, we started to investigate the encoding of high beat frequencies and found significant spike time locking of P-units to beat frequencies up to 500 Hz (Sinz et al., 2017). These data seem to parallel spike time locking to amplitude modulations described in the peripheral vertebrate auditory systems (Joris et al., 2004) and might explain how high beat frequencies are reliably represented, as the courtship behaviors that we observed suggest. Future studies need to explore these coding schemes, in particular with respect to the encoding of chirps occurring on beat frequencies beyond 250 Hz.

The difference between the high beat frequencies that we observed during courtship interactions (205–415 Hz; Figs. 8*F*, 4*B*) and the peak of the frequency tuning of the firing rate (Fig. 8*H*) is unexpected given the many examples of frequency-matched courtship signals in other sensory systems (Rieke et al., 1995; Machens et al., 2005; Kostarakos et al., 2009; Schrode and Bee, 2015). The high beat frequencies result from males having higher frequencies than females (Meyer et al., 1987). In the genus *Apteronotus*, the presence, magnitude, and direction of EOD*f* dimorphism varies considerably across species and thus is evolutionarily labile (Smith, 2013).

Neglected stimulus amplitudes

The field strength of the EOD, and with it beat amplitude, decays with distance (Fig. 8*A*). Most of the studies on P-unit coding, including Savard et al. (2011) and Sinz et al. (2017), used rather strong beat amplitudes of >10% of the EOD amplitude. We observed chirp interactions at distances up to 32 cm, corresponding to beat amplitudes of ~1% (Fig. 8*A*). Opponent assessment and decision to attack usually occur at even larger distances (Fig. 8*C*), where the relevant signal amplitudes are much smaller than 1% of the fish's own EOD amplitude. In general, smaller beat amplitudes result in down-scaled frequency tuning curves (Bastian, 1981a; Benda et al., 2006; Savard et al., 2011; Grewe et al., 2017) and reduced phase locking (Sinz et al., 2017). However, encoding of beats and chirps has so far only been studied for amplitudes larger than 1% (Bastian, 1981a; Nelson et al., 1997).

Decoding

P-units converge onto pyramidal cells in the electrosensory lateral line lobe (ELL) (Heiligenberg and Dye, 1982; Maler, 2009). The rate tuning curves of pyramidal cells peak at frequencies similar to or lower than those of P-units (Bastian, 1981b) and their stimulus–response coherences peak well below 100 Hz, but have only been measured up to 120 Hz (Chacron et al., 2003; Chacron, 2006; Krahe et al., 2008). In contrast to the auditory system, where phase locking to amplitude modulations in neurons of the cochlear nucleus is improved relative to auditory nerve fibers (Joris et al., 2004), phase locking in pyramidal cells compared with P-unit afferents is reduced (Sinz et al., 2017). Coding of small chirps by pyramidal cells in the ELL and at the next stage of processing, the torus semicircularis, has so far only been studied at beat frequencies below 60 Hz (Marsat et al., 2009; Marsat and Maler, 2010; Vonderschen and Chacron, 2011; Marsat et al., 2012; Metzen et al., 2016). Therefore, most electrophysiological recordings from the electrosensory system have been biased to low beat frequencies and strong stimulus amplitudes evoking obvious neuronal responses, but overlooking the stimuli relevant for reproduction.

Conclusion

Our observations regarding sex specificity, numbers, and functions of chirps differ substantially from laboratory studies. The fish robustly responded to courtship signals that occurred on beat frequencies that were unexpectedly high given previous, mainly laboratory-based findings on chirping (Smith, 2013; Walz et al., 2013). In addition, male fish initiated attacks at distances resulting in unexpectedly low beat amplitudes. These ranges of stimulus frequencies and amplitudes have been largely ignored by electrophysiological characterizations of the electrosensory system. Our field data thus identify important, but so far neglected, stimulus regimes of the electrosensory system and provide further evidence for the existence of sensitive neural mechanisms for the detection of such difficult sensory signals (Gao and Ganguli, 2015). Our work also points to the limitations of laboratory studies and emphasizes the importance of research in the natural habitat, which opens new windows for understanding the real challenges faced and solved by sensory systems.

References

Arnott G, Elwood RW (2008) Information gathering and decision making about resource value in animal contests. Anim Behav 76:529–542. CrossRef

Bastian J (1981a) Electrolocation I. How electroreceptors of *Apteronotus albifrons* code for moving objects and other electrical stimuli. J Comp Physiol 144:465–479. CrossRef

Bastian J (1981b) Electrolocation II. The effects of moving objects and other electrical stimuli on the activities of two categories of posterior lateral line lobe cells in *Apteronotus albifrons.* J Comp Physiol 144:481–494. CrossRef

Bastian J, Schniederjan S, Nguyenkim J (2001) Arginine vasotocin modulates a sexually dimorphic communication behavior in the weakly electric fish *Apteronotus leptorhynchus.* J Exp Biol 204:1909–1923. Medline

Benda J, Longtin A, Maler L (2005) Spike-frequency adaptation separates transient communication signals from background oscillations. J Neurosci 25:2312–2321. CrossRef Medline

Benda J, Longtin A, Maler L (2006) A synchronization-desynchronization code for natural communication signals. Neuron 52:347–358. CrossRef Medline

Bullock TH, Hamstra RH, Scheich H (1972) The jamming avoidance response of high frequency electric fish. II. Quantitative aspects. J Comp Physiol 77:23–48. CrossRef

Carr CE, Maler L, Sas E (1982) Peripheral organization and central projections of the electrosensory nerves in gymnotiform fish. J Comp Neurol 211:139–153. CrossRef Medline

Chacron MJ (2006) Nonlinear information processing in a model sensory system. J Neurophysiol 95:2933–2946. CrossRef Medline

Chacron MJ, Doiron B, Maler L, Longtin A, Bastian J (2003) Non-classical receptive field mediates switch in a sensory neuron's frequency tuning. Nature 423:77–81. CrossRef Medline

Clemens J, Ronacher B (2013) Feature extraction and integration underlying perceptual decision making during courtship behavior. J Neurosci 33:12136–12145. CrossRef Medline

de Santana CD, Vari RP (2013) Brown ghost electric fishes of the *Apteronotus leptorhynchus* species-group (Ostariophysi, Gymnotiformes); monophyly, major clades, and revision. Zool J Linnean Soc 168:564–596. CrossRef

Egnor SE, Branson K (2016) Computational analysis of behavior. Annu Rev Neurosci 39:217–236. CrossRef Medline

Endler JA (1993) Some general comments on the evolution and design of animal communication systems. Philos Trans R Soc Lond B Biol Sci 340: 215–225. CrossRef Medline

Engler G, Zupanc GK (2001) Differential production of chirping behavior evoked by electrical stimulation of the weakly electric fish, *Apteronotus leptorhynchus.* J Comp Physiol A 187:747–756. CrossRef Medline

Fotowat H, Harrison RR, Krahe R (2013) Statistics of the electrosensory input in the freely swimming weakly electric fish *Apteronotus leptorhynchus.* J Neurosci 33:13758–13772. CrossRef Medline

Froudarakis E, Berens P, Ecker AS, Cotton RJ, Sinz FH, Yatsenko D, Saggau P, Bethge M, Tolias AS (2014) Population code in mouse V1 facilitates readout of natural scenes through increased sparseness. Nat Neurosci 17:851–857. CrossRef Medline

Fugère V, Ortega H, Krahe R (2011) Electrical signalling of dominance in a wild population of electric fish. Biol Lett 7:197–200. CrossRef Medline

Gao P, Ganguli S (2015) On simplicity and complexity in the brave new world of large-scale neuroscience. Curr Opin Neurobiol 32:148–155. CrossRef Medline

Gollisch T, Meister M (2010) Eye smarter than scientists believed: neural computations in circuits of the retina. Neuron 65:150–164. CrossRef Medline

Grewe J, Kruscha A, Lindner B, Benda J (2017) Synchronous spikes are necessary but not sufficient for a synchrony code in populations of spiking neurons. Proc Natl Acad Sci U S A 114:E1977–E1985. CrossRef Medline

Hagedorn M, Heiligenberg W (1985) Court and spark: electric signals in the courtship and mating of gymnotid fish. Anim Behav 33:254–265. CrossRef

Heiligenberg W, Dye J (1982) Labelling of electroreceptive afferents in a gymnotoid fish by intraeellular injection of HRP: the mystery of multiple maps. J Comp Physiol 148:287–296. CrossRef

Henninger J (2015) Social interactions in natural populations of weakly electric fish. PhD dissertation, Eberhard Karls Universität Tübingen.

Hopkins CD (1973) Lightning as background noise for communication among electric fish. Nature 242:268–270. CrossRef

Hupé GJ, Lewis JE (2008) Electrocommunication signals in free swimming brown ghost knifefish, *Apteronotus leptorhynchus.* J Exp Biol 211:1657–1667. CrossRef Medline

Joris PX, Schreiner CE, Rees A (2004) Neural processing of amplitude-modulated sounds. Physiol Rev 84:541–577. CrossRef Medline

Kirschbaum F, Schugardt C (2002) Reproductive strategies and developmental aspects in mormyrid and gymnotiform fishes. J Physiol Paris 96: 557–566. CrossRef Medline

Knudsen EI (1974) Behavioral thresholds to electric signals in high frequency electric fish. J Comp Physiol A Neuroethol Sens Neural Behav Physiol 91:333–353.

Kostarakos K, Hennig MR, Römer H (2009) Two matched filters and the evolution of mating signals in four species of cricket. Front Zool 6:22. CrossRef Medline

Krahe R, Bastian J, Chacron MJ (2008) Temporal processing across multiple topographic maps in the electrosensory system. J Neurophysiol 100:852–867. CrossRef Medline

Laughlin S (1981) A simple coding procedure enhances a neuron's information capacity. Z Naturforsch C 36:910–912. Medline

Lewicki MS, Olshausen BA, Surlykke A, Moss CF (2014) Scene analysis in the natural environment. Front Psychol 5:199. CrossRef Medline

Machens CK, Gollisch T, Kolesnikova O, Herz AV (2005) Testing the efficiency of sensory coding with optimal stimulus ensembles. Neuron 47: 447–456. CrossRef Medline

Maler L (2009) Receptive field organization across multiple electrosensory maps. I. Columnar organization and estimation of receptive field size. J Comp Neurol 516:376–393. CrossRef Medline

Marsat G, Maler L (2010) Neural heterogeneity and efficient population codes for communication signals. J Neurophysiol 104:2543–2555. CrossRef Medline

Marsat G, Proville RD, Maler L (2009) Transient signals trigger synchronous bursts in an identified population of neurons. J Neurophysiol 102: 714–723. CrossRef Medline

Marsat G, Longtin A, Maler L (2012) Cellular and circuit properties supporting different sensory coding strategies in electric fish and other systems. Curr Opin Neurobiol 22:686–692. CrossRef Medline

Metzen MG, Chacron MJ (2017) Stimulus background influences phase invariant coding by correlated neural activity. eLife 6:e24482. CrossRef Medline

Metzen MG, Hofmann V, Chacron MJ (2016) Neural correlations enable invariant coding and perception of natural stimuli in weakly electric fish. eLife 5:e12993. CrossRef Medline

Meyer JH, Leong M, Keller CH (1987) Hormone-induced and maturational changes in electric organ discharges and electroreceptor tuning in the weakly electric fish *Apteronotus.* J Comp Physiol A 160:385–394. CrossRef Medline

Nelson ME, Maciver MA (1999) Prey capture in the weakly electric fish *Apteronotus albifrons*: sensory acquisition strategies and electrosensory consequences. J Exp Biol 202:1195–1203. Medline

Nelson ME, Xu Z, Payne JR (1997) Characterization and modeling of P-type electrosensory afferent responses to amplitude modulations in a wave-type electric fish. J Comp Physiol A 181:532–544. CrossRef Medline

Olshausen BA, Field DJ (1996) Emergence of simple-cell receptive-field properties by learning a sparse code for natural images. Nature 381:607–609. CrossRef Medline

Olshausen BA, Field DJ (2005) How close are we to understanding V1? Neural Comput 17:1665–1699. CrossRef Medline

Rieke F, Bodnar DA, Bialek W (1995) Naturalistic stimuli increase the rate and efficiency of information transmission by primary auditory afferents. Proc Biol Sci 262:259–265. CrossRef Medline

Rose G, Heiligenberg W (1985) Temporal hyperacuity in the electric sense of fish. Nature 318:178–180. CrossRef Medline

Salgado JAG, Zupanc GKH (2011) Echo response to chirping in the weakly electric brown ghost knifefish (*Apteronotus leptorhynchus*): role of frequency and amplitude modulations. Can J Zool 89:498–508. CrossRef

Savard M, Krahe R, Chacron MJ (2011) Neural heterogeneities influence envelope and temporal coding at the sensory periphery. Neuroscience 172:270–284. CrossRef Medline

Scheich H, Bullock TH, Hamstra RH J (1973) Coding properties of two classes of afferent nerve fibers: high frequency electroreceptors in the electric fish, *Eigenmannia.* J Neurophysiol 36:39–60. CrossRef Medline

Schrode KM, Bee MA (2015) Evolutionary adaptations for the temporal processing of natural sounds by the anuran peripheral auditory system. J Exp Biol 218:837–848. CrossRef Medline

Sinz FH, Sachgau C, Henninger J, Benda J, Grewe J (2017) Simultaneous spike time locking to multiple frequencies. bioRxiv. CrossRef

Smith EC, Lewicki MS (2006) Efficient auditory coding. Nature 439:978–982. CrossRef Medline

Smith GT (2013) Evolution and hormonal regulation of sex differences in the electrocommunication behavior of ghost knifefishes (Apteronotidae). J Exp Biol 216:2421–2433. CrossRef Medline

Stamper SA, Carrera-G E, Tan EW, Fugère V, Krahe R, Fortune ES (2010) Species differences in group size and electrosensory interference in weakly electric fishes: implications for electrosensory processing. Behav Brain Res 207:368–376. CrossRef Medline

Theunissen FE, Sen K, Doupe AJ (2000) Spectral-temporal receptive fields of nonlinear auditory neurons obtained using natural sounds. J Neurosci 20:2315–2331. CrossRef Medline

Triefenbach FA, Zakon H (2008) Changes in signalling during agonistic interactions between male weakly electric knifefish, *Apteronotus leptorhynchus.* Anim Behav 75:1263–1272. CrossRef

Vonderschen K, Chacron MJ (2011) Sparse and dense coding of natural stimuli by distinct midbrain neuron subpopulations in weakly electric fish. J Neurophysiol 106:3102–3118. CrossRef Medline

Walz H, Hupé GJ, Benda J, Lewis JE (2013) The neuroethology of electrocommunication: how signal background influences sensory encoding and behaviour in *Apteronotus leptorhynchus.* J Physiol Paris 107:13–25. CrossRef Medline

Walz H, Grewe J, Benda J (2014) Static frequency tuning properties account for changes in neural synchrony evoked by transient communication signals. J Neurophysiol 112:752–765. CrossRef Medline

Wilson EO (1975) Sociobiology: the new synthesis. Cambridge, MA: Harvard University.

Zakon H, Oestreich J, Tallarovic S, Triefenbach F (2002) EOD modulations of brown ghost electric fish: JARs, chirps, rises, and dips. J Physiol Paris 96:451–458. CrossRef Medline

Zupanc GK, Sîrbulescu RF, Nichols A, Ilies I (2006) Electric interactions through chirping behavior in the weakly electric fish, *Apteronotus leptorhynchus.* J Comp Physiol A Neuroethol Sens Neural Behav Physiol 192: 159–173. CrossRef Medline